

Cyclic Pyrrole–Imidazole Polyamides Targeted to the Androgen Response Element

David M. Chenoweth, Daniel A. Harki, John W. Phillips, Christian Dose, and Peter B. Dervan*

Division of Chemistry and Chemical Engineering, California Institute of Technology, Pasadena, California 91125

Received February 19, 2009; E-mail: dervan@caltech.edu

Abstract: Hairpin pyrrole–imidazole (Py–Im) polyamides are a class of cell-permeable DNA-binding small molecules that can disrupt transcription factor–DNA binding and regulate endogenous gene expression. The covalent linkage of antiparallel Py–Im ring pairs with an γ -amino acid turn unit affords the classical hairpin Py–Im polyamide structure. Closing the hairpin with a second turn unit yields a cyclic polyamide, a lesser-studied architecture mainly attributable to synthetic inaccessibility. We have applied our methodology for solution-phase polyamide synthesis to cyclic polyamides with an improved high-yield cyclization step. Cyclic 8-ring Py–Im polyamides **1–3** target the DNA sequence 5′-WGWWCW-3′, which corresponds to the androgen response element (ARE) bound by the androgen receptor transcription factor to modulate gene expression. We find that cyclic Py–Im polyamides **1–3** bind DNA with exceptionally high affinities and regulate the expression of AR target genes in cell culture studies, from which we infer that the cycle is cell permeable.

Introduction

Modulating the expression of eukaryotic gene networks by small molecules is a challenge at the frontier of chemical biology. Pyrrole–imidazole polyamides are a class of cell-permeable small molecules that bind to the minor groove of DNA in a sequence-specific manner.^{1,2} Side-by-side stacked *N*-methylpyrrole (Py) and *N*-methylimidazole (Im) carboxamides (Im/Py pairs) distinguish G•C from C•G base pairs, whereas Py/Py pairs specify for both T•A and A•T.³ Py–Im hairpin polyamides have been programmed for a broad repertoire of DNA sequences with affinities similar to those of endogenous transcription factors.⁴ They are cell permeable and influence gene transcription by disrupting protein–DNA interfaces.^{2,5,6} Hairpin polyamide interference of DNA binding by transcription factors such as HIF-1 α ,⁷ androgen receptor (AR),⁸ and AP-1⁹ has been described in recent years, yielding a new approach toward gene control by small molecules.

In parallel with our gene regulation studies, a significant effort has been devoted to maximizing the biological potency of hairpin Py–Im polyamides through structural modifications. In particular, we have recently demonstrated that hairpin polyamides bearing the (*R*)- β -amino- γ -turn, such as polyamide **4**, possess favorable binding affinities to DNA and are useful in

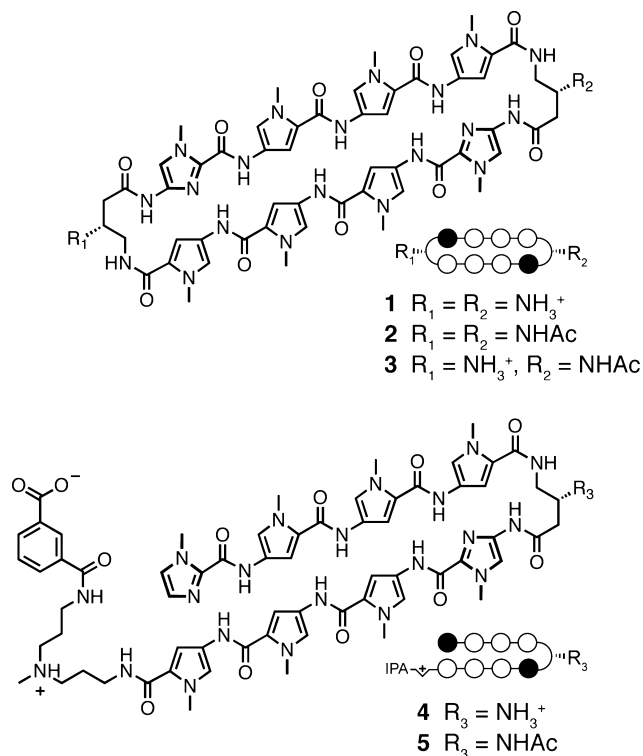


Figure 1. Structures of cyclic and hairpin polyamides **1–5** targeted to the DNA sequence 5′-WGWWCW-3′ and their ball-and-stick models. Black and white circles represent *N*-methylimidazole and *N*-methylpyrrole units, respectively, IPA denotes the terminal isophthalic acid substituent, and white half-diamond with + sign represents the triamine linker unit.

gene regulation studies (Figure 1).^{5g} A significant effort exists in our laboratory to regulate aberrant AR-activated gene

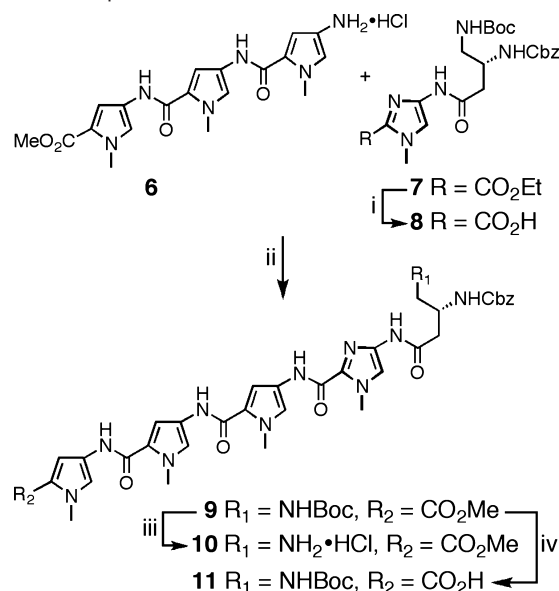
- (1) Dervan, P. B. *Bioorg. Med. Chem.* **2001**, *9*, 2215–2235.
- (2) Dervan, P. B.; Edelson, B. S. *Curr. Opin. Struct. Biol.* **2003**, *13*, 284–299.
- (3) (a) Trauger, J. W.; Baird, E. E.; Dervan, P. B. *Nature* **1996**, *382*, 559–561. (b) White, S.; Szewczyk, J. W.; Turner, J. M.; Baird, E. E.; Dervan, P. B. *Nature* **1998**, *391*, 468–470. (c) Kielkopf, C. L.; Baird, E. E.; Dervan, P. B.; Rees, D. C. *Nat. Struct. Biol.* **1998**, *5*, 104–109. (d) Kielkopf, C. L.; White, S.; Szewczyk, J. W.; Turner, J. M.; Baird, E. E.; Dervan, P. B.; Rees, D. C. *Science* **1998**, *282*, 111–115.
- (4) Hsu, C. F.; Phillips, J. W.; Trauger, J. W.; Farkas, M. E.; Belitsky, J. M.; Heckel, A.; Olenyuk, B. Z.; Puckett, J. W.; Wang, C. C. C.; Dervan, P. B. *Tetrahedron* **2007**, *63*, 6146–6151.

expression in prostate cancer.⁸ To further optimize lead oligomer **4**, it would seem reasonable that closing the hairpin with an identical linker, yielding a cyclic structure **1**, would further enhance DNA affinity (Figure 1). Previous syntheses of cyclic polyamides using solid-phase protocols are characterized by low reaction yields due to inefficient macrocyclization.¹⁰ We report here the solution-phase synthesis of cyclic polyamides **1–3** with an improved high-yield cyclization step. In addition, we examined the DNA binding properties of these compounds by thermal duplex DNA melting and performed preliminary studies of their *in vitro* ADMET properties. Cyclic Py-Im polyamides **1–3** were shown to regulate endogenous gene expression in cell culture experiments.

Results and Discussion

Solution-Phase Synthesis of Cyclic Polyamides. Due to the symmetrical nature of cyclic polyamides **1–3** and their sequence similarity to previously described hairpin polyamide **4**,¹¹ PyPyPy trimer **6** and Im-turn dimer **7** provide all the necessary atoms to synthesize **1–3**. The preparation of advanced intermediates **6** and **7** has been detailed in the preceding paper (DOI 10.1021/ja901307m)¹¹ from readily available building blocks.¹² The cornerstone of our synthesis strategy capitalizes on the disparate physical properties of starting materials versus products, which permit purification of most intermediates to be achieved by

Scheme 1. Preparation of **10** and **11**^a



^a Reagents and conditions: (i) M KOH(aq), MeOH, 37 °C, 2 h, 95%; (ii) **8**, PyBOP, DMF, DIEA, **6**, 23 °C, 4 h, 96%; (iii) 4.0 M HCl in 1,4-dioxane, 23 °C, 2 h, 99%; (iv) M NaOH(aq), 1,4-dioxane, 42 °C, 3 h, 95%.

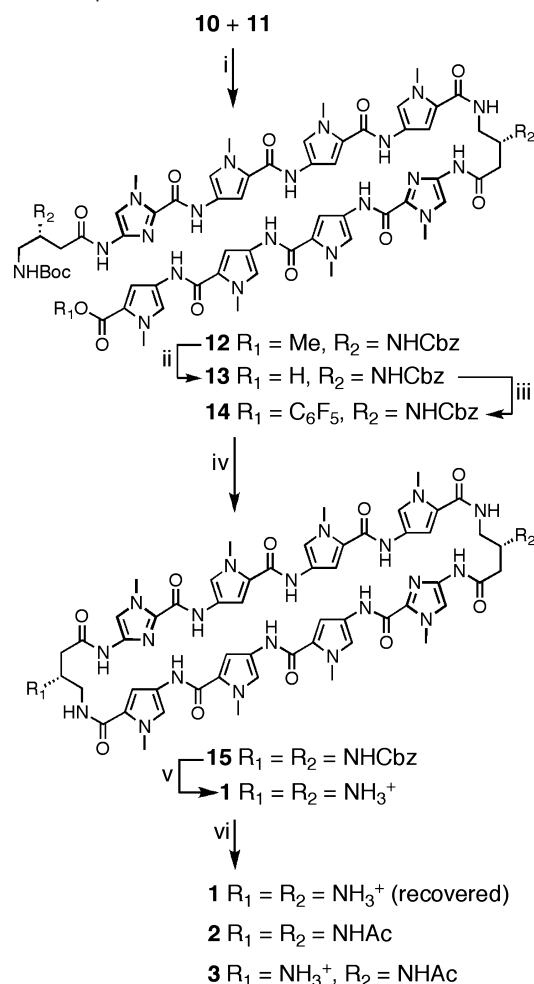
combinations of precipitation, trituration, and crystallization. In addition, *in situ* deprotection of advanced pentafluorophenyl ester polyamide **14** at high dilution leads to macrocyclization in high yield, affording cyclic polyamide **15**.

The synthesis of tetramer-turn **9** begins with Im-turn dimer **7** (Scheme 1). Saponification of **7** with aqueous KOH in methanol at 37 °C, followed by neutralization, precipitation, and Et₂O trituration, yields Im-turn acid **8** in 95% yield. Amide coupling of **8** with pyrrole trimer **6** provides pentamer **9** in 96% yield. The utilization of a small excess of **6** relative to **8** drives the reaction to completion, and residual **6** is readily separated from **9** following precipitation in water and aqueous washing of residual solid **9**. With all atoms in place for the target cyclic polyamide **1**, compound **9** was elaborated to amine salt **10** (99% yield) by reaction with HCl in 1,4-dioxane. Carboxylic acid **11** was generated by saponification of **9** with NaOH in 1,4-dioxane in 95% yield.

Assembly of the acyclic advanced intermediate **12** was achieved by PyBOP-mediated coupling of intermediates **10** and **11** in 94% yield (Scheme 2). A small excess of amine salt **10** was utilized to drive the reaction to completion. Saponification of ester **12** proceeded smoothly with aqueous NaOH in 1,4-dioxane, yielding **13** in 93% yield. Activation of acid **13** as the pentafluorophenol ester **14** provided the necessary functionality to afford macrocyclization following removal of the terminal *tert*-butyl carbamate (Boc) protecting group. In our hands, we found that the pentafluorophenol ester sufficiently activated the terminal acid for amide coupling while avoiding undesired oligomerization and/or decomposition processes that are conceivable with more reactive functionalities, such as acid chlorides. Premature initiation of the macrocyclization reaction was tempered by keeping the terminal amine protonated until it was transferred into a dilute solution of acetonitrile. Addition

- (5) (a) Belitsky, J. M.; Leslie, S. J.; Arora, P. S.; Beerman, T. A.; Dervan, P. B. *Bioorg. Med. Chem.* **2002**, *10*, 3313–3318. (b) Crowley, K. S.; Phillion, D. P.; Woodard, S. S.; Scheitzer, B. A.; Singh, M.; Shabany, H.; Burnette, B.; Hippenmeyer, P.; Heitmeier, M.; Bashkin, J. K. *Bioorg. Med. Chem. Lett.* **2003**, *13*, 1565–1570. (c) Best, T. P.; Edelson, B. S.; Nickols, N. G.; Dervan, P. B. *Proc. Natl. Acad. Sci. U.S.A.* **2003**, *100*, 12063–12068. (d) Edelson, B. S.; Best, T. P.; Olenyuk, B.; Nickols, N. G.; Doss, R. M.; Foister, S.; Heckel, A.; Dervan, P. B. *Nucleic Acids Res.* **2004**, *32*, 2802–2818. (e) Xiao, X.; Yu, P.; Lim, H. S.; Sikder, D.; Kodadek, T. *Angew. Chem., Int. Ed.* **2007**, *46*, 2865–2868. (f) Nickols, N. G.; Jacobs, C. S.; Farkas, M. E.; Dervan, P. B. *Nucleic Acids Res.* **2007**, *35*, 363–370. (g) Dose, C.; Farkas, M. E.; Chenoweth, D. M.; Dervan, P. B. *J. Am. Chem. Soc.* **2008**, *130*, 6859–6866. (h) Hsu, C. F.; Dervan, P. B. *Bioorg. Med. Chem. Lett.* **2008**, *18*, 5851–5855.
- (6) (a) Gottesfeld, J. M.; Melander, C.; Suto, R. K.; Raviol, H.; Luger, K.; Dervan, P. B. *J. Mol. Biol.* **2001**, *309*, 615–629. (b) Suto, R. K.; Edayathumangalam, R. S.; White, C. L.; Melander, C.; Gottesfeld, J. M.; Dervan, P. B.; Luger, K. *J. Mol. Biol.* **2003**, *326*, 371–380. (c) Edayathumangalam, R. S.; Weyermann, P.; Gottesfeld, J. M.; Dervan, P. B.; Luger, K. *Proc. Natl. Acad. Sci. U.S.A.* **2004**, *101*, 6864–6869. (d) Dudouet, B.; Burnett, R.; Dickinson, L. A.; Wood, M. R.; Melander, C.; Belitsky, J. M.; Edelson, B.; Wurtz, N.; Briehn, C.; Dervan, P. B.; Gottesfeld, J. M. *Chem. Biol.* **2003**, *10*, 859–867.
- (7) (a) Olenyuk, B. Z.; Zhang, G. J.; Klco, J. M.; Nickols, N. G.; Kaelin Jr., W. G.; Dervan, P. B. *Proc. Natl. Acad. Sci. U.S.A.* **2004**, *101*, 16768–16773. (b) Kageyama, Y.; Sugiyama, H.; Ayame, H.; Iwai, A.; Fujii, Y.; Huang, L. E.; Kizaka-Kondoh, S.; Hiraoka, M.; Kihara, K. *Acta Oncol.* **2006**, *45*, 317–324. (c) Nickols, N. G.; Jacobs, C. S.; Farkas, M. E.; Dervan, P. B. *ACS Chem. Biol.* **2007**, *2*, 561–571.
- (8) Nickols, N. G.; Dervan, P. B. *Proc. Natl. Acad. Sci. U.S.A.* **2007**, *104*, 10418–10423.
- (9) (a) Matsuda, H.; Fukuda, N.; Ueno, T.; Tahira, Y.; Ayame, H.; Zhang, W.; Bando, T.; Sugiyama, H.; Saito, S.; Matsumoto, K.; et al. *J. Am. Soc. Nephrol.* **2006**, *17*, 422–432. (b) Yao, E. H.; Fukuda, N.; Ueno, T.; Matsuda, H.; Matsumoto, K.; Nagase, H.; Matsumoto, Y.; Takasaka, A.; Serie, K.; Sugiyama, H.; Sawamura, T. *Hypertension* **2008**, *52*, 86–92.
- (10) (a) Cho, J.; Parks, M. E.; Dervan, P. B. *Proc. Natl. Acad. Sci. U.S.A.* **1995**, *92*, 10389–10392. (b) Zhang, Q.; Dwyer, T. J.; Tsui, V.; Case, D. A.; Cho, J.; Dervan, P. B.; Wemmer, D. E. *J. Am. Chem. Soc.* **2004**, *126*, 7958–7966. (c) Herman, D. M.; Turner, J. M.; Baird, E. E.; Dervan, P. B. *J. Am. Chem. Soc.* **1999**, *121*, 1121–1129. (d) Melander, C.; Herman, D. M.; Dervan, P. B. *Chem.—Eur. J.* **2000**, *6*, 4487–4497.
- (11) Chenoweth, D. M.; Harki, D. A.; Dervan, P. B. *J. Am. Chem. Soc.* **2009**, *131*, <http://dx.doi.org/10.1021/ja901307m>.

- (12) (a) Baird, E. E.; Dervan, P. B. *J. Am. Chem. Soc.* **1996**, *118*, 6141–6146. (b) Wurtz, N. R.; Turner, J. M.; Baird, E. E.; Dervan, P. B. *Org. Lett.* **2001**, *3*, 1201–1203. (c) Jaramillo, D.; Liu, Q.; Aldrich-Wright, J.; Tor, Y. *J. Org. Chem.* **2004**, *69*, 8151–8153.

Scheme 2. Preparation of **1**, **2**, and **3**^a

^a Reagents and conditions: (i) PyBOP, DMF, DIEA, 23°C, 2 h, 94%; (ii) NaOH(aq), 1,4-dioxane, 40°C, 4 h, 93%; (iii) CH_2Cl_2 , DCC, pentafluorophenol, DMAP, 23°C, 12 h, 80%; (iv) a) TFA, CH_2Cl_2 , 23°C, concentrate; b) DMF, acetonitrile, DIEA, 0–23°C, 3 days; (v) $\text{CF}_3\text{SO}_3\text{H}$, $\text{CF}_3\text{CO}_2\text{H}$, 23°C, 5 min, 68% over 3 steps; (vi) NMP, DIEA, Ac_2O , 23°C, 18% of **1** (recovered), 22% of **2**, 40% of **3**.

of an amine base (DIEA) then generated the free terminal amine, which could then undergo macrocyclization in dilute solvent conditions to deliver **15**, which was directly deprotected following purification. The benzyl carbamate protecting groups were cleaved by treatment with superacid conditions (trifluoromethylsulfonic acid–trifluoroacetic acid) to provide **1** in 68% yield over three steps. Controlled acetylation of **1** by reaction with substoichiometric quantities of Ac_2O in NMP/DIEA provided a statistical population of **1** (18%), **2** (22%), and **3** (40%) that were easily separable by preparative HPLC. Acetylated hairpin **5** was prepared using excess Ac_2O /pyridine in 95% yield from previously reported amine hairpin **4**.¹¹

Thermal Stabilization of DNA Duplexes by Polyamides. Quantitative DNase I footprint titrations have historically been utilized to measure polyamide–DNA binding affinities and specificities.¹³ However, this method is limited to measuring K_a values $\leq 2 \times 10^{10} \text{ M}^{-1}$, which invalidates this technique for quantifying the exceptionally high DNA-binding affinities of cycles **1**–**3**.¹⁴ The magnitude of DNA thermal stabilization

Table 1. T_m Values for Polyamides for **1**–**5**^a

Polyamides	$T_m / ^\circ\text{C}$	$\Delta T_m / ^\circ\text{C}$
—	60.0 (± 0.3)	—
$\text{H}_3\text{N}^+ \cdots \text{NH}_3^+$ (1)	83.5 (± 0.5)	23.6 (± 0.6)
AcHN \cdots NHAc (2)	81.2 (± 0.2)	21.3 (± 0.4)
$\text{H}_3\text{N}^+ \cdots \text{NHAc}$ (3)	82.0 (± 0.0)	22.1 (± 0.3)
IPA \cdots NH_3^+ (4)	78.4 (± 0.5)	18.4 (± 0.6)
IPA \cdots NHAc (5)	76.0 (± 0.5)	16.1 (± 0.6)

^a All values reported are derived from at least three melting temperature experiments with standard deviations indicated in parentheses. ΔT_m values are given as $T_m^{\text{(DNA/polyamide)}} - T_m^{\text{(DNA)}}$. The propagated error in ΔT_m measurements is the square root of the sum of the square of the standard deviations for the T_m values.

(ΔT_m) of DNA–polyamide complexes has been utilized to rank order polyamides with high DNA binding affinities.^{5g,15} Accordingly, we have employed melting temperature analysis (ΔT_m) for dissecting differences in DNA-binding affinities of hairpin versus cyclic polyamides. Spectroscopic analyses were performed on a 14-mer duplex DNA mimicking the androgen response element (ARE) DNA sequence, 5'-TTGCTGTTCT-GCAA-3' DNA duplex, which contains one polyamide binding site. As shown in Table 1, polyamides **1**–**5** provided an increase in the duplex DNA melting temperature relative to the individual DNA duplex, thereby confirming polyamide–DNA binding. Chiral hairpin **4** led to an increased melting temperature, $\Delta T_m = 18.4 ^\circ\text{C}$, whereas cyclic polyamide **1** yielded a higher ΔT_m value of 23.6 $^\circ\text{C}$. Cyclic polyamides **1**–**3** reveal stronger stabilizations than parent hairpin analogues **4** and **5**. Acylation of the β -amino turns was shown to decrease the thermal stabilization values in both hairpin and cyclic motifs, presumably due to the loss of the electrostatic benefit of the cation-protonated amine on the turn unit.

Biological Assay for Cell Permeability. Hairpin polyamides have been shown to modulate endogenous gene expression in living cells by disrupting transcription factor–DNA binding in gene promoters.^{2,7–9} Recently, hairpin polyamide **4** was shown to inhibit androgen receptor-mediated expression of prostate-specific antigen (PSA) in LNCaP cells by targeting the DNA

(14) For examples of polyamides with K_a values $> 2 \times 10^{10} \text{ M}^{-1}$ and a discussion of the limitations of quantitative DNase I footprint titrations, please refer to ref 5g. A polyamide analogous to **4**, ImPyPyPy-(R) $^{\beta\text{-H}_2\text{N}}\gamma$ -ImPyPyPy- β -Dp, was found to have $K_a > 2 \times 10^{10} \text{ M}^{-1}$.^{5g} Additionally, previous studies with cyclic polyamide *cyclo*-(–ImPyPyPy-(R) $^{\alpha\text{-H}_2\text{N}}\gamma$ -ImPyPyPy- γ –) found K_a values far exceeding $2 \times 10^{10} \text{ M}^{-1}$ by DNase I footprint titrations.^{10c,d} Cyclic polyamide **1** possesses dual β -amino functionalities, a modification that yields even greater DNA binding affinities compared with α -amino and unsubstituted γ -turns for hairpin polyamides of sequence ImPyPyPy- γ -ImPyPyPy.^{5g} The DNA binding affinity of **1** most likely supersedes that of predecessor *cyclo*-(–ImPyPyPy-(R) $^{\alpha\text{-H}_2\text{N}}\gamma$ -ImPyPyPy- γ –).

(15) (a) Pilch, D. S.; Poklar, N.; Gelfand, C. A.; Law, S. M.; Breslauer, K. J.; Baird, E. E.; Dervan, P. B. *Proc. Natl. Acad. Sci. U.S.A.* **1996**, *93*, 8306–8311. (b) Pilch, D. S.; Poklar, N.; Baird, E. E.; Dervan, P. B.; Breslauer, K. J. *Biochemistry* **1999**, *38*, 2143–2151.

(13) Trauger, J. W.; Dervan, P. B. *Methods Enzymol.* **2001**, *340*, 450–466.

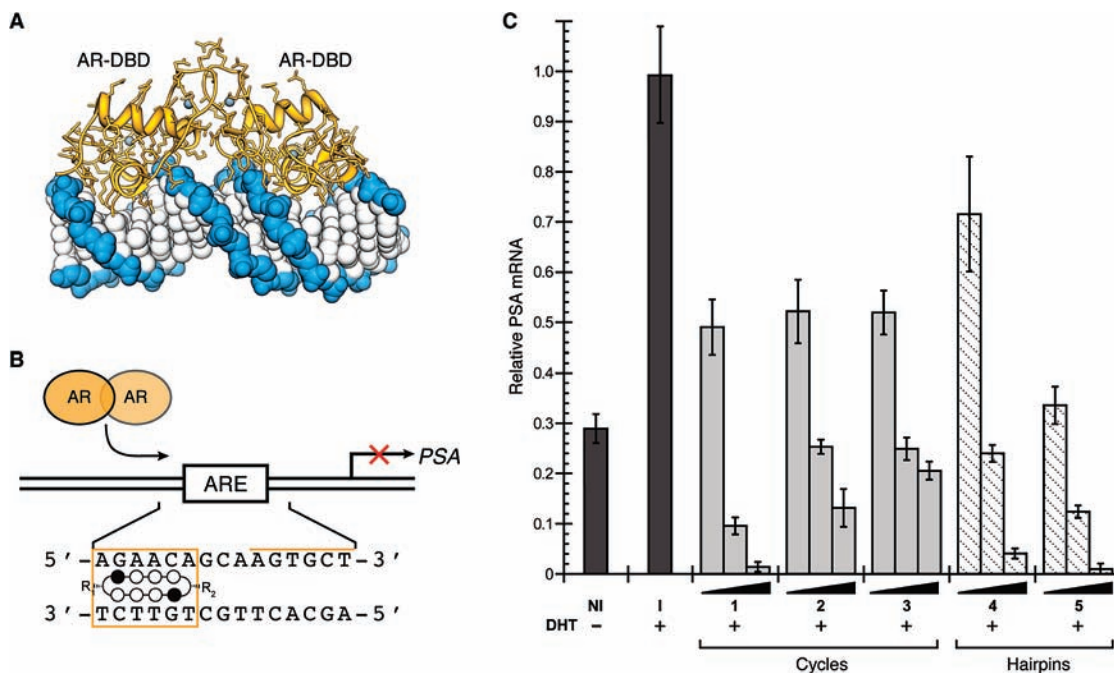


Figure 2. Targeting the ARE with DNA-binding polyamides. (a) X-ray crystal structure of androgen receptor homodimer DNA-binding domain bound to the sequence 5'-CTGTTCTTGATGTTCTGG-3' (PDB 1r4i).¹⁶ (b) Map of the PSA-ARE site (top) and schematic representation of a cyclic polyamide targeting the PSA-ARE site 5'-AGAACA-3'. (c) Inhibition of induced PSA mRNA expression in LNCaP cells by cyclic Py-Im polyamides **1–3** and hairpin polyamides **4** and **5** (dosed at 0.3, 3, and 30 μM) by real-time quantitative PCR. The results were normalized to a DHT-induced, untreated control (control = 1), and the error bars represent the standard error of the mean of a single experiment performed in biological triplicate. The entire experiment was reproduced four times, with similar results. NI = noninduced, I = induced, DHT = dihydrotestosterone.

sequence 5'-AGAACA-3' found in the ARE.^{5g} We utilized this cell culture transcription assay to investigate the biological activity of cyclic polyamides **1–3** in comparison to hairpin polyamides **4** and **5**. Since small structural changes to polyamides have been shown to correlate with differences in cellular uptake properties,⁵ it was not obvious whether cyclic polyamides **1–3** would permeate cell membranes and exhibit biological activity comparable to that of hairpin polyamides **4** and **5**. Quantitative real-time RT-PCR analysis of DHT-induced PSA expression revealed that cyclic polyamides **1–3** all decreased PSA mRNA levels in LNCaP cells, with cycle **1** exhibiting activity comparable to that of acetylated hairpin polyamide **5** (Figure 2). On the basis of these results, we can infer that this class of cyclic Py-Im polyamides are cell permeable and can regulate endogenous gene expression in cell culture.

ADMET Studies of Polyamides **1 and **5**.** Due to the promising cell culture results obtained with cyclic polyamide **1** and hairpin polyamide **5** against PSA gene expression, we contracted preclinical *in vitro* absorption, distribution, metabolism, excretion, and toxicity (ADMET)¹⁷ studies for both compounds.¹⁸ Results from this study are summarized below, and additional detail can be found in the Supporting Information. Polyamides **1** and **5** were both found to exhibit low Caco-2 permeability, suggesting that neither compound may be orally available. Both **1** and **5** were found to be almost exclusively protein bound in plasma, with half-lives greater than 2 h. A recent positron emission tomography (PET)-based biodistribution study of a

related hairpin polyamide in mice revealed high levels of liver occupancy following tail vein dosage.¹⁹ On the basis of this result, we investigated the liver stability of candidate polyamides **1** and **5**. Microsomal intrinsic clearance studies found half-lives greater than 3 h for **1** and **5** in both human and rat liver microsomes, and no significant inhibition was measured against any cytochrome P450 isoform examined (Cyp1A2/CEC, Cyp2C8/DBF, Cyp2C9/DBF, Cyp2C19/DBF, Cyp2D6/AMMC, Cyp3A4/BFC, Cyp3A4/DBF). Furthermore, no obvious toxicity ($\text{IC}_{50} > 100 \mu\text{M}$) was observed in the human hepatocellular carcinoma cell line HepG2. In addition, standard hERG FastPatch assays of cardiac toxicity found that both polyamides (**1** and **5**) were devoid of unwanted inhibition ($\text{IC}_{50} > 100 \mu\text{M}$).

Conclusion

We describe a solution-phase synthesis methodology for preparing cyclic Py-Im polyamides, highlighted by an efficient macrocyclization between the alkyl linker amine and a pentafluorophenol ester-activated amino acid. The three cyclic Py-Im polyamides possessed high DNA-binding affinities and were capable of accessing the nucleus in cell culture, as judged by their ability to downregulate AR-activated PSA expression in cell culture. Preclinical ADMET analysis of cyclic polyamide **1** and hairpin polyamide **5** revealed favorable drug-like properties such as high liver stability and low toxicity. Ongoing work is focused on characterizing the precise molecular interactions between cyclic polyamides and their cognate DNA sequences by high-resolution crystallographic studies.

Experimental Section

General. Chemicals and solvents were purchased from Sigma-Aldrich and were used without further purification. (*R*)-3,4-Cbz-

(16) Shaffer, P. L.; Jivan, A.; Dollins, D. E.; Claessens, F.; Gewirth, D. T. *Proc. Natl. Acad. Sci. U.S.A.* **2004**, *101*, 4758–4763.

(17) For a review of pharmacokinetics in drug discovery, see: Ruiz-Garcia, A.; Bermejo, M.; Moss, A.; Casabo, V. G. *J. Pharm. Sci.* **2008**, *97*, 654–690.

(18) Apredica, 313 Pleasant St., Watertown, MA 02472 (<http://www.apredica.com/>).

(19) Harki, D. A.; Satyamurthy, N.; Stout, D. B.; Phelps, M. E.; Dervan, P. B. *Proc. Natl. Acad. Sci. U.S.A.* **2008**, *105*, 13039–13044.

Dbu(Boc)-OH was purchased from Senn Chemicals AG (code number 44159). All DNA oligomers were purchased HPLC purified from Integrated DNA Technologies. Water (18 M Ω) was purified using a Millipore Milli-Q purification system. Centrifugation was performed in a Beckman Coulter benchtop centrifuge (Allegra 21R) equipped with a Beckman swing-out rotor (model S4180). Analytical HPLC analysis was conducted on a Beckman Gold instrument equipped with a Phenomenex Gemini analytical column (250 \times 4.6 mm, 5 μ m) and a diode array detector, and the mobile phase consisted of a gradient of acetonitrile (MeCN) in 0.1% (v/v) aqueous CF₃CO₂H. Preparative HPLC was performed on an Agilent 1200 system equipped with a solvent degasser, a diode array detector, and a Phenomenex Gemini column (250 \times 21.2 mm, 5 μ m). A gradient of MeCN in 0.1% (v/v) aqueous CF₃CO₂H was utilized as the mobile phase. UV-vis measurements were made on a Hewlett-Packard diode array spectrophotometer (model 8452 A), and polyamide concentrations were measured in 0.1% (v/v) aqueous CF₃CO₂H using an extinction coefficient of 69 200 M⁻¹ cm⁻¹ at λ_{max} near 310 nm. NMR spectroscopy was performed on a Varian instrument operating at 499.8 (for ¹H) or 125.7 MHz (for ¹³C) at ambient temperature. All NMR analyses were performed in DMSO-*d*₆, and chemical shifts are reported in parts per million relative to the internal solvent peak referenced to 2.49 (for ¹H) or 39.5 (for ¹³C). High-resolution mass spectrometry (HRMS) was recorded in positive-ion mode by fast-atom bombardment (FAB⁺) on a JEOL JMS-600H instrument or by electrospray ionization (ESI⁺) on a Waters Acquity UPLC-LCT Premiere XE TOF-MS system.

UV Absorption Spectrophotometry. Melting temperature analysis was performed on a Varian Cary 100 spectrophotometer equipped with a thermo-controlled cell holder possessing a cell path length of 1 cm. A degassed aqueous solution of 10 mM sodium cacodylate, 10 mM KCl, 10 mM MgCl₂, and 5 mM CaCl₂ at pH 7.0 was used as analysis buffer. DNA duplexes and polyamides were mixed in 1:1 stoichiometry to a final concentration of 2 μ M for each experiment. Prior to analysis, samples were heated to 90 °C and cooled to a starting temperature of 23 °C with a heating rate of 5 °C/min for each ramp. Denaturation profiles were recorded at $\lambda = 260$ nm from 23 to 90 °C with a heating rate of 0.5 °C/min. The reported melting temperatures were defined as the maximum of the first derivative of the denaturation profile.

Measurement of Androgen-Induced PSA mRNA. Experiments were performed as described previously⁸ with the following modifications: (1) all compounds and controls were prepared in neat DMSO and then diluted with media to a final concentration of 0.1% DMSO, and (2) mRNA was isolated with the RNEasy 96 kit (Qiagen, Valencia, CA).

BocHN-(R) ^{β} -CbzHN γ -Im-CO₂H (8). A solution of BocHN-(R) ^{β} -CbzHN γ -Im-CO₂Et **7** (450 mg, 0.894 mmol) dissolved in MeOH (1.0 mL) and aqueous KOH (1 N, 2.0 mL, 2.0 mmol) was stirred at 37 °C for 2 h. The reaction mixture was added to a cooled (ice bath) solution of distilled H₂O (10 mL) preacidified with aqueous HCl (1 N, 2.0 mL, 2.0 mmol), yielding a precipitate that was isolated by centrifugation (~4500 rpm). The residual solid was again suspended in distilled H₂O (10 mL) and collected by centrifugation. The resultant solid, which contained a small amount of residual H₂O, was frozen and lyophilized to dryness and then suspended in excess anhydrous Et₂O and filtered, and the filter cake washed with copious amounts of anhydrous Et₂O. Drying of the brown solid *in vacuo* yielded saponified dimer **8** (404 mg, 95%). ¹H NMR: δ 10.46 (s, 1H), 7.47 (s, 1H), 7.31–7.26 (m, 5H), 7.02 (d, $J = 8.3$ Hz, 1H), 6.79 (t, $J = 5.4$ Hz, 1H), 4.97 (s, 2H), 3.92 (m, 1H), 3.88 (s, 3H), 3.60 (s, 1H), 3.01 (m, 2H), 2.41 (m, 2H), 1.35 (s, 9H). ¹³C NMR: δ 167.6, 160.0, 155.8, 155.4, 137.11, 137.09, 131.6, 128.2, 127.66, 127.55, 114.6, 77.7, 65.1, 48.7, 43.5, 38.0, 35.4, 28.2. HRMS (FAB⁺): calcd for C₂₂H₃₀N₅O₇ [M + H]⁺, 476.2145; found, 476.2130.

BocHN-(R) ^{β} -CbzHN γ -ImPyPyPy-CO₂Me (9). A solution of BocHN-(R) ^{β} -CbzHN γ -Im-CO₂H **8** (300 mg, 0.631 mmol) and PyBOP (345 mg, 0.663 mmol) in DMF (3.2 mL) and DIEA (330 μ L, 1.9 mmol)

was stirred at 23 °C for 10 min. The solution was then treated with solid (powdered) HCl·H₂N-PyPyPy-CO₂Me **6** (288 mg, 0.663 mmol) and stirred at 23 °C for 4 h. The solution was then added to distilled H₂O (10 mL) preacidified with aqueous HCl (1 N, 2 mL, 2 mmol), yielding a precipitate that was isolated by centrifugation (~4500 rpm). The residual solid was again suspended in distilled H₂O (10 mL) and collected by centrifugation (repeated 3 \times). The resultant solid, which contained a small amount of residual H₂O, was frozen and lyophilized to dryness. The solid was triturated with anhydrous Et₂O and filtered over a sintered glass funnel. The resultant solid was washed with copious amounts of anhydrous Et₂O and dried *in vacuo* to yield BocHN-(R) ^{β} -CbzHN γ -ImPyPyPy-CO₂Me **9** as a tan solid (518 mg, 96%). ¹H NMR: δ 10.17 (s, 1H), 10.00 (s, 1H), 9.95 (s, 1H), 9.93 (s, 1H), 7.46 (d, $J = 1.7$ Hz, 1H), 7.44 (s, 1H), 7.31–7.29 (m, 5H), 7.27 (d, $J = 1.7$ Hz, 1H), 7.23 (d, $J = 1.7$ Hz, 1H), 7.14 (d, $J = 1.7$ Hz, 1H), 7.07 (d, $J = 1.7$ Hz, 1H), 7.04 (d, $J = 8.3$ Hz, 1H), 6.90 (d, $J = 2.0$ Hz, 1H), 6.81 (t, $J = 5.9$ Hz, 1H), 4.98 (s, 2H), 3.96 (m, 1H), 3.95 (s, 3H), 3.85 (s, 3H), 3.84 (s, 3H), 3.83 (s, 3H), 3.73 (s, 3H), 3.03 (m, 2H), 2.46 (m, 2H), 1.36 (s, 9H). ¹³C NMR: δ 167.8, 160.8, 158.5, 158.4, 155.84, 155.81, 155.5, 137.1, 136.0, 134.0, 128.3, 127.7, 127.6, 123.06, 123.00, 122.5, 122.2, 121.2, 120.7, 118.7, 118.6, 118.5, 114.0, 108.4, 104.9, 77.8, 65.2, 50.9, 48.8, 43.6, 38.2, 36.20, 36.18, 36.09, 34.9, 28.2. HRMS (FAB⁺): calcd for C₄₁H₄₉N₁₁O₁₀ [M]⁺, 855.3663; found, 855.3688.

HCl·H₂N-(R) ^{β} -CbzHN γ -ImPyPyPy-CO₂Me (10). A solution of BocHN-(R) ^{β} -CbzHN γ -ImPyPyPy-CO₂Me **9** (125 g, 0.146 mmol) in anhydrous HCl in 1,4-dioxane (4.0 M, 10 mL) was stirred at 23 °C for 2 h. The mixture was then diluted with 100 mL of anhydrous Et₂O and filtered over a sintered glass funnel. The resultant solid was washed with copious amounts of anhydrous Et₂O and dried *in vacuo* to yield HCl·H₂N-(R) ^{β} -CbzHN γ -ImPyPyPy-CO₂Me **10** as a brown solid (114 mg, 99%). ¹H NMR: δ 10.38 (s, 1H), 9.98 (s, 1H), 9.96 (s, 1H), 9.94 (s, 1H), 8.10 (m, 3H), 7.46 (d, $J = 1.7$ Hz, 1H), 7.45 (s, 1H), 7.42 (d, $J = 8.3$ Hz, 1H), 7.34–7.28 (m, 5H), 7.28 (d, $J = 1.7$ Hz, 1H), 7.24 (d, $J = 1.7$ Hz, 1H), 7.16 (d, $J = 1.7$ Hz, 1H), 7.08 (d, $J = 1.7$ Hz, 1H), 6.90 (d, $J = 1.7$ Hz, 1H), 5.02 (m, 2H), 4.14 (m, 1H), 3.95 (s, 3H), 3.85 (s, 3H), 3.84 (s, 3H), 3.83 (s, 3H), 3.73 (s, 3H), 3.02 (m, 2H), 2.63 (m, 2H). ¹³C NMR: δ 167.0, 160.8, 158.5, 158.4, 155.7, 136.8, 135.7, 134.0, 128.3, 127.8, 127.7, 123.05, 122.97, 122.5, 122.2, 121.1, 120.7, 118.64, 118.60, 118.5, 108.4, 104.9, 65.6, 50.9, 46.7, 42.0, 38.2, 36.2, 36.1, 36.0, 34.9. HRMS (FAB⁺): calcd for C₃₆H₄₂N₁₁O₈ [M + H]⁺, 756.3218; found, 756.3211.

BocHN-(R) ^{β} -CbzHN γ -ImPyPyPy-CO₂H (11). A solution of BocHN-(R) ^{β} -CbzHN γ -ImPyPyPy-CO₂Me **9** (200 mg, 0.234 mmol) dissolved in 1,4-dioxane (2.3 mL) and aqueous NaOH (1 N, 2.3 mL, 2.3 mmol) was stirred at 42 °C for 3 h. The solution was then added to distilled H₂O (5 mL) preacidified with aqueous HCl (1 N, 2.3 mL, 2.3 mmol), yielding a precipitate that was isolated by centrifugation (~4500 rpm). The residual solid was again suspended in distilled H₂O (10 mL) and collected by centrifugation (repeated 2 \times). The resultant solid, which contained a small amount of residual H₂O, was frozen and lyophilized to dryness and then suspended in excess anhydrous Et₂O and filtered, and the filter cake washed with copious amounts of anhydrous Et₂O. Drying of the tan solid *in vacuo* yielded BocHN-(R) ^{β} -CbzHN γ -ImPyPyPy-CO₂H **11** (187 mg, 95%). ¹H NMR: δ 12.15 (s, 1H), 10.21 (s, 1H), 10.00 (s, 1H), 9.96 (s, 1H), 9.92 (s, 1H), 7.44 (s, 1H), 7.42 (d, $J = 1.7$ Hz, 1H), 7.31–7.29 (m, 5H), 7.28 (d, $J = 1.5$ Hz, 1H), 7.24 (d, $J = 1.5$ Hz, 1H), 7.16 (d, $J = 1.5$ Hz, 1H), 7.08 (m, 2H), 6.85 (d, $J = 1.7$ Hz, 1H), 6.82 (t, $J = 5.7$ Hz, 1H), 4.98 (s, 2H), 3.95 (m, 4H), 3.85 (s, 3H), 3.84 (s, 3H), 3.81 (s, 3H), 3.03 (m, 2H), 2.46 (m, 2H), 1.36 (s, 9H). ¹³C NMR: δ 167.8, 162.0, 158.44, 158.38, 155.80, 155.77, 155.4, 137.1, 136.0, 133.9, 128.3, 127.7, 127.6, 123.0, 122.7, 122.6, 122.2, 121.2, 120.2, 119.5, 118.6, 118.5, 114.0, 108.4, 104.87, 104.83, 77.7, 65.1, 48.8, 43.5, 38.2, 36.2, 36.13, 36.06, 34.9, 28.2. HRMS (FAB⁺): calcd for C₄₀H₄₇N₁₁O₁₀ [M]⁺, 841.3507; found, 841.3498.

BocHN-(R)^β-CbzHN γ -ImPyPyPy-(R)^β-CbzHN γ -ImPyPyPy-CO₂Me (12). A solution of BocHN-(R)^β-CbzHN γ -ImPyPyPy-CO₂H **11** (25 mg, 0.029 mmol) and PyBOP (17 mg, 0.031 mmol) in DMF (150 μ L) and DIEA (16 μ L, 0.089 mmol) was stirred at 23 °C for 20 min. The solution was then treated with solid (powdered) HCl·H₂N-(R)^β-CbzHN γ -ImPyPyPy-CO₂Me **10** (25 mg, 0.031 mmol) and stirred at 23 °C for 2 h. The solution was then added to distilled H₂O (10 mL) preacidified with aqueous HCl (1 N, 1 mL, 1 mmol), yielding a precipitate that was isolated by centrifugation (~4500 rpm). The residual solid was again suspended in distilled H₂O (10 mL) and collected by centrifugation (repeated 3 \times). The resultant solid, which contained a small amount of residual H₂O, was frozen and lyophilized to dryness. The solid was triturated with anhydrous Et₂O and filtered over a sintered glass funnel. The resultant solid was washed with copious amounts of anhydrous Et₂O and dried *in vacuo* to yield BocHN-(R)^β-CbzHN γ -ImPyPyPy-(R)^β-CbzHN γ -ImPyPyPy-CO₂Me **12** as a tan solid (44 mg, 94%). ¹H NMR: δ 10.20 (s, 1H), 10.16 (s, 1H), 9.98 (s, 2H), 9.94–9.91 (m, 4H), 7.99 (m, 1H), 7.46 (d, *J* = 1.7 Hz, 1H), 7.45 (s, 1H), 7.44 (s, 1H), 7.32–7.14 (m, 18H), 7.07 (m, 2H), 7.03 (d, *J* = 8.3 Hz, 1H), 6.92 (s, 1H), 6.90 (d, *J* = 2.0 Hz, 1H), 6.80 (t, *J* = 5.6 Hz, 1H), 4.99 (m, 4H), 4.10 (m, 1H), 3.95 (m, 7H), 3.85–3.83 (m, 15H), 3.79 (s, 3H), 3.73 (s, 3H), ~3.30 (m, 2H, obstructed by H₂O peak), 3.04 (m, 2H), 2.53–2.44 (m, 4H, partially obstructed by NMR solvent), 1.36 (s, 9H). ¹³C NMR: δ 167.9, 167.8, 161.6, 160.8, 158.5, 158.44, 158.42, 155.8, 155.6, 155.5, 137.1, 136.0, 134.00, 133.98, 128.3, 127.7, 127.63, 127.60, 123.11, 123.07, 123.00, 122.80, 122.77, 122.5, 122.3, 122.2, 122.1, 121.3, 120.8, 118.69, 118.66, 118.62, 118.52, 118.0, 114.1, 108.4, 104.9, 104.8, 104.5, 77.8, 65.21, 65.16, 50.9, 48.83, 48.78, 43.6, 42.2, 38.4, 38.2, 36.2, 36.10, 36.07, 36.0, 34.9, 28.2. HRMS (TOF-ESI⁺): calcd for C₇₆H₈₇N₂₂O₁₇ [M + H]⁺, 1579.6620; found, 1579.6580.

BocHN-(R)^β-CbzHN γ -ImPyPyPy-(R)^β-CbzHN γ -ImPyPyPy-CO₂H (13). A solution of BocHN-(R)^β-CbzHN γ -ImPyPyPy-(R)^β-CbzHN γ -ImPyPyPy-CO₂Me **12** (25 mg, 0.0158 mmol) dissolved in 1,4-dioxane (376 μ L) and aqueous NaOH (1 N, 253 μ L, 0.253 mmol) was stirred at 40 °C for 4 h. The solution was then added to distilled H₂O (5 mL) preacidified with aqueous HCl (1 N, 253 μ L, 0.253 mmol), yielding a precipitate that was diluted with another 15 mL of H₂O and was then isolated by centrifugation (~4500 rpm). The resultant solid, which contained a small amount of residual H₂O, was frozen and lyophilized to dryness and then suspended in excess anhydrous Et₂O, triturated, and filtered, and the filter cake washed with copious amounts of anhydrous Et₂O. Drying of the tan solid *in vacuo* yielded BocHN-(R)^β-CbzHN γ -ImPyPyPy-(R)^β-CbzHN γ -ImPyPyPy-CO₂H **13** (23 mg, 93%). ¹H NMR: δ 12.13 (br s, 1H), 10.23 (s, 1H), 10.20 (s, 1H), 9.98–9.90 (m, 6H), 8.01 (m, 1H), 7.443 (s, 1H), 7.439 (s, 1H), 7.42 (d, *J* = 1.7 Hz, 1H), 7.30–7.15 (m, 18H), 7.07 (m, 3H), 6.92 (m, 1H), 6.84 (d, *J* = 2.0 Hz, 1H), 6.81 (t, *J* = 5.6 Hz, 1H), 5.00 (m, 2H), 4.98 (s, 2H), 4.10 (m, 1H), 3.95 (m, 7H), 3.85–3.83 (m, 12H), 3.81 (s, 3H), 3.78 (s, 3H), ~3.30 (m, 2H, obstructed by H₂O peak), 3.03 (m, 2H), 2.53 (m, 2H), 2.46 (m, 2H), 1.36 (s, 9H). ¹³C NMR: δ 167.94, 167.87, 162.4, 162.0, 161.6, 158.54, 158.50, 158.43, 155.8, 155.75, 155.74, 155.6, 155.5, 137.1, 136.0, 133.91, 133.90, 128.3, 127.7, 127.60, 127.57, 123.10, 123.07, 122.8, 122.7, 122.6, 122.3, 122.24, 122.17, 121.16, 121.15, 120.3, 119.5, 118.64, 118.61, 118.5, 118.0, 114.10, 114.06, 108.5, 105.0, 104.5, 77.8, 65.2, 65.1, 48.8, 43.6, 42.2, 38.4, 38.2, 36.2, 36.14, 36.10, 36.08, 36.0, 35.8, 34.9, 28.2. HRMS (TOF-ESI⁺): calcd for C₇₅H₈₆N₂₂O₁₇ [M + 2H]²⁺/2, 783.3271; found, 783.3237.

BocHN-(R)^β-CbzHN γ -ImPyPyPy-(R)^β-CbzHN γ -ImPyPyPy-CO₂Pfp (14). A solution of BocHN-(R)^β-CbzHN γ -ImPyPyPy-(R)^β-CbzHN γ -ImPyPyPy-CO₂H **13** (250 mg, 0.160 mmol) and DCC (66 mg, 0.320 mmol) in CH₂Cl₂ (8.8 mL) was stirred at 23 °C for 45 min. The solution was then treated with DMAP (2 mg, 0.016 mmol) followed by pentafluorophenol (175 mg, 0.950 mmol) and stirred at 23 °C for 12 h. The reaction mixture was then loaded onto a silica gel column with CH₂Cl₂ and eluted with step gradients of 100% CH₂Cl₂ to 100% acetone with incremental steps of 5%

acetone. The product was concentrated *in vacuo* to yield BocHN-(R)^β-CbzHN γ -ImPyPyPy-(R)^β-CbzHN γ -ImPyPyPy-CO₂Pfp **14** as a brown solid (221 mg, 80%). ¹H NMR: δ 10.20 (s, 1H), 10.16 (s, 1H), 10.08 (s, 1H), 9.99–9.91 (m, 5H), 7.99 (m, 1H), 7.73 (d, *J* = 1.7 Hz, 1H), 7.444 (s, 1H), 7.440 (s, 1H), 7.30–7.12 (m, 20 H), 7.06 (d, *J* = 1.2 Hz, 1H), 7.03 (d, *J* = 8.5 Hz, 1H), 6.92 (s, 1H), 6.80 (t, *J* = 5.4 Hz, 1H), 5.00 (m, 2H), 4.98 (m, 2H), 4.11 (m, 1H), 3.95 (m, 7H), 3.88 (s, 3H), 3.86–3.84 (m, 12H), 3.78 (s, 3H), ~3.30 (m, 2H, obstructed by H₂O peak), 3.04 (m, 2H), 2.52 (m, 2H), 2.46 (m, 2H), 1.36 (s, 9H). HRMS (TOF-ESI⁺): calcd for C₈₁H₈₅F₅N₂₂O₁₇ [M + 2H]²⁺/2, 866.3192; found, 866.3236.

cyclo-(–ImPyPyPy-(R)^β-H₂N γ -ImPyPyPy-(R)^β-H₂N γ –) (1). A solution of BocHN-(R)^β-CbzHN γ -ImPyPyPy-(R)^β-CbzHN γ -ImPyPyPy-CO₂Pfp **14** (84 mg, 0.049 mmol) in anhydrous CF₃CO₂H:CH₂Cl₂ (1:1, 4 mL) was stirred at 23 °C for 10 min prior to being concentrated to dryness in a 500 mL round-bottom flask. The residue was then dissolved in cold (0 °C) DMF (10 mL), followed by immediate dilution with MeCN (300 mL) and DIEA (1.6 mL). The reaction mixture was left at 23 °C for 3 days without stirring. [Note: The solution turns cloudy as the macrocyclization proceeds.] The reaction mixture was concentrated to a volume of 11 mL and added to a solution of H₂O (30 mL) and aqueous HCl (1 N, 9.2 mL) at 0 °C. The protected intermediate *cyclo*-(–ImPyPyPy-(R)^β-CbzHN γ -ImPyPyPy-(R)^β-CbzHN γ –) **15** was isolated by centrifugation (~4500 rpm), lyophilized to dryness, and then suspended in excess anhydrous Et₂O, triturated, and filtered, and the filter cake washed with copious amounts of anhydrous Et₂O. Drying of the tan solid *in vacuo* yielded the protected intermediate *cyclo*-(–ImPyPyPy-(R)^β-CbzHN γ -ImPyPyPy-(R)^β-CbzHN γ –) **15**. HRMS (TOF-ESI⁺): calcd for C₇₀H₇₆N₂₂O₁₄ [M + 2H]²⁺/2, 724.2956; found, 724.2925. This material was immediately deprotected by dissolving in CF₃CO₂H (2 mL) followed by addition of CF₃SO₃H (100 μ L) at 23 °C for 5 min. The solution was then frozen, and DMF (2 mL) was layered over the frozen solution. The thawed solution was diluted with H₂O (6 mL) and purified by reverse-phase HPLC to give a white solid after lyophilization. The solid was suspended in excess anhydrous Et₂O, triturated, and filtered, and the filter cake was washed with copious amounts of anhydrous Et₂O. Drying of the white solid *in vacuo* yielded *cyclo*-(–ImPyPyPy-(R)^β-H₂N γ -ImPyPyPy-(R)^β-H₂N γ –) **1** (46 mg, 68%). ¹H NMR: δ 10.56 (s, 2H), 9.91 (s, 4H), 9.88 (s, 2H), 8.17 (t, *J* = 5.6 Hz, 2H), 7.96 (m, 6H), 7.40 (s, 2H), 7.31 (d, *J* = 1.6 Hz, 2H), 7.27 (d, *J* = 1.6 Hz, 2H), 7.19 (d, *J* = 1.6 Hz, 2H), 7.00 (d, *J* = 1.7 Hz, 2H), 6.96 (d, *J* = 1.6 Hz, 2H), 6.94 (d, *J* = 1.7 Hz, 2H), 3.94 (s, 6H), 3.83 (s, 12H), 3.80 (s, 6H), 3.71–3.66 (m, 2H), 3.49–3.27 (m, 4H, partially obstructed by H₂O peak), 2.79 (dd, *J* = 16.1 Hz, 6.0 Hz, 2H), 2.60 (dd, *J* = 15.2 Hz, 5.2 Hz, 2H). HRMS (TOF-ESI⁺): calcd for C₅₄H₆₃N₂₂O₁₀ [M + H]⁺, 1179.5098; found, 1179.5087.

cyclo-(–ImPyPyPy-(R)^β-AcHN γ -ImPyPyPy-(R)^β-H₂N γ –) (3) and cyclo-(–ImPyPyPy-(R)^β-AcHN γ -ImPyPyPy-(R)^β-AcHN γ –) (2). A solution of *cyclo*-(–ImPyPyPy-(R)^β-H₂N γ -ImPyPyPy-(R)^β-H₂N γ –) **1** (2.81 mg, 2.0 μ mol) in anhydrous NMP (200 μ L) and DIEA (20 μ L) at 23 °C was treated with a solution of Ac₂O in NMP (0.122 M, 6.8 μ L). After 10 min, the reaction mixture was treated with another 6.8 μ L of Ac₂O in NMP (0.122 M) and allowed to stand for 5 h. The reaction mixture was then diluted to a volume of 10 mL by addition of a 4:1 solution of aqueous CF₃CO₂H (0.1% v/v):MeCN (5 mL), followed by additional aqueous CF₃CO₂H (0.1% v/v, 5 mL), and then purified by reverse-phase HPLC to yield *cyclo*-(–ImPyPyPy-(R)^β-H₂N γ -ImPyPyPy-(R)^β-H₂N γ –) **1** (363 nmol, 18%), *cyclo*-(–ImPyPyPy-(R)^β-AcHN γ -ImPyPyPy-(R)^β-H₂N γ –) **3** (800 nmol, 40%), and *cyclo*-(–ImPyPyPy-(R)^β-AcHN γ -ImPyPyPy-(R)^β-AcHN γ –) **2** (432 nmol, 22%). For *cyclo*-(–ImPyPyPy-(R)^β-AcHN γ -ImPyPyPy-(R)^β-H₂N γ –) **3**, HRMS (TOF-ESI⁺): calcd for C₅₆H₆₅N₂₂O₁₁ [M + H]⁺, 1221.5203; found, 1221.5204. For *cyclo*-(–ImPyPyPy-(R)^β-AcHN γ -ImPyPyPy-(R)^β-AcHN γ –) **2**, HRMS (TOF-ESI⁺): calcd for C₅₈H₆₈N₂₂O₁₂ [M + 2H]²⁺/2, 633.2646; found, 633.2631.

ImPyPyPy-(R)^β-H₂N γ -ImPyPyPy-(+)-IPA (4). Prepared as described in the preceding paper.¹¹

ImPyPyPy-(R)^β-AcHN-γ-ImPyPyPy-(+)-IPA (5). A solution of polyamide **4**¹¹ (7.4 mg, 5.03 μmol, assumes **4** as the mono-CF₃CO₂H salt) in DMF (1.76 mL) was treated with a solution of Ac₂O in pyridine (10% v/v, 240 μL, 0.254 mmol of Ac₂O). The solution was allowed to stand at 23 °C for 30 min and then acidified with aqueous CF₃CO₂H (15% v/v, 2 mL). After 5 min the solution was further diluted with distilled H₂O (5 mL), purified by preparative RP-HPLC, and lyophilized to dryness. Suspension of the residual solid in anhydrous Et₂O, following by filtration and drying under high vacuum, yielded **5** (6.7 mg, 95%). HRMS (FAB⁺): calcd for C₆₇H₇₉N₂₂O₁₃ [M + H]⁺, 1399.6191; found, 1399.6181.

Acknowledgment. This work was supported by the National Institutes of Health (GM27681). DMC is grateful for a Caltech Kanel predoctoral fellowship. DAH thanks the California Tobacco-Related Disease Research Program (16FT-0055) for a postdoctoral

fellowship. JWP is grateful to the California Breast Cancer Research Program for a predoctoral fellowship. CD thanks the Alexander von Humboldt foundation for a postdoctoral research fellowship. The National Science Foundation Chemistry Research Instrumentation and Facilities Program (CHE-0541745) is acknowledged for providing the UPLC-MS instrument.

Supporting Information Available: Summary of ADMET results, ¹H and ¹³C NMR spectra, and analytical HPLC purity analyses of selected compounds. This material is available free of charge via the Internet at <http://pubs.acs.org>. The full ADMET report including experimental conditions can be accessed via the Dervan laboratory homepage at <http://dervan.caltech.edu>.

JA901309Z